Generating the Highest Power with a Tiny and Distant Inductively Coupled Coil

Nan Xing, *Graduate Student Member, IEEE,* and Gabriel A. Rincón-Mora, *Fellow, IEEE*
Georgia Institute of Technology, Atlanta, Georgia 30332 U.S.A.
nxing3@gatech.edu and Rincon-Mora@gatech.edu

Abstract—**Although microsystems today require less power than ever before, they still cannot fit large enough batteries to sustain them for months or years at a time. Ambient energy is appealing, but only when available, which is often not the case for embedded sensors. Transmitting power wirelessly is more practical in these applications. Tiny receivers, however, capture a small fraction of the power that a distant source can deliver. So output power is low and its effects on the transmitting coil are barely noticeable. Receivers should therefore draw as much power as possible, but only as much as breakdown voltages and power losses allow. This paper shows that, although the switched bridge can draw 27% more power than resonant bridges, synchronization and ohmic losses negate that gain. In fact, breakdown voltages limit the switched resonant bridge less than others in the state of the art. Plus, the switched resonant bridge excludes the charger that the others require for maximum output power, so with less space and less added losses, power density can be greater.**

Index Terms—Wireless power transfer, inductively coupled power receiver, maximum output power, damping force, battery charger, biomedical implant, and embedded microsensor.

I. Wirelessly-Powered Microsystems

Although microwatt microsystems can sense, process, and report information [1]–[3] that can save lives, energy, and money, tiny onboard batteries cannot sustain them for long [4]. Energy in light, motion, and thermal gradients can help [5], but only when available. Unfortunately, ambient energy in embedded biomedical and structural devices is often scarce, so coupling power wirelessly is the only recourse left [6]–[8].

In these cases, feeding alternating current into a transmitting coil L_T like Fig. 1 shows produces a changing magnetic field from which a nearby receiving coil L_R can draw power. The changing flux induces an electromotive-force (EMF) voltage $v_{EMF.R}$ that can supply power. But since L_R in embedded sensors can be centimeters away from L_T, L_R receives a low fraction k_C^2 of the power L_T can deliver, which is why $v_{EMF.R}$ is normally in millivolts [9]–[10].

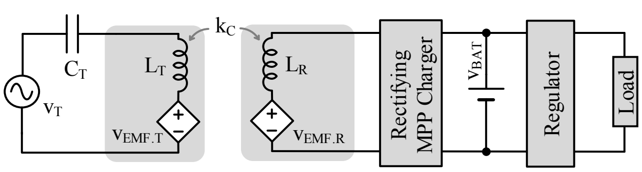

Fig. 1. Inductively powered system.

Since $v_{EMF.R}$ outputs so little power, a rectifying maximum power-point (MPP) charger draws just enough power into the battery v_{BAT} to keep the receiver at its maximum power point. v_{BAT} then caches this energy until the load requires it. The purpose of the regulator is to supply and condition the power that the load demands.

This paper assesses how the state of the art in inductively coupled power receivers can draw and output the highest power possible from tiny coils that are centimeters away from their transmitting sources. For this, Section II first reviews how to draw power from small coils. Sections III, IV, and IV then review and evaluate how bridges draw and output power. Sections V and VI end with comparisons and conclusions.

II. Drawing Electromagnetic Power

To understand how $v_{EMF.R}$ in Fig. 1 generates power, first consider that impressing $v_{EMF.R}$'s sinusoid across L_R produces a current $i_{L(0)}$ in Fig. 2 that is 90° out of phase. This results because $v_{EMF.R}$'s positive half cycles raise i_L and $v_{EMF.R}$'s negative half cycles reduce i_L about a 0-mA median. $v_{EMF.R}$ and $i_{L(0)}$ are therefore both positive and both negative half the time and opposite polarities the other half. This means, $v_{EMF.R}$ outputs as much power as it consumes, so output power is nil.

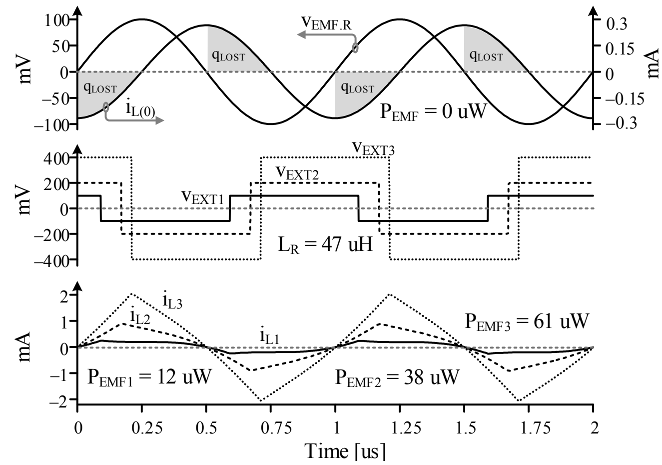

Fig. 2. Simulated waveforms with and without an external voltage v_{EXT}.

The only way to net output power is to reduce the phase difference between $v_{EMF.R}$ and i_L. Luckily, applying an external voltage v_{EXT} at the beginning of $v_{EMF.R}$'s positive half cycle like Fig. 2 shows at 0 μs energizes L_R quicker to a higher peak i_L so that applying a negative voltage after that can help reduce i_L to zero at the end of the half cycle. Similarly, applying a negative v_{EXT} when the negative half cycle begins at 0.5 μs energizes L_R to a lower peak i_L so that impressing a positive voltage after that can help raise i_L to zero at the end of the half cycle. When balanced this way, $v_{EMF.R}$ and i_L are in phase (with the same polarity), so $v_{EMF.R}$ only *sources* power.

If the system is lossless, v_{EXT} recovers the power that v_{EXT} delivers with i_L. In other words, v_{EXT} receives what $v_{EMF.R}$ produces. And since a higher v_{EXT} raises i_L to an even higher peak, higher v_{EXT}'s can draw more power from $v_{EMF.R}$. This is why v_{EXT1}'s 100 mV, v_{EXT2}'s 200 mV, and v_{EXT3}'s 400 mW in Fig. 2 draw 12, 38, and 61 µW, respectively. The rectifying MPP charger in Fig. 1 must therefore apply across L_R the highest voltage possible that keeps $v_{EMF.R}$ and i_L in phase.

III. Resonant Bridges

A. Resonant Half Bridge

Paralleling a capacitor C_R across L_R in Fig. 3 produces a voltage v_C across C_R that, when tuned to $v_{EMF.R}$'s operating frequency f_O, crosses zero between $v_{EMF.R}$'s half cycles (similar in phase to v_{EXT3} from Fig. 2). So when first energized, $v_{EMF.R}$ supplies more power than it consumes, and L_R and C_R receive and exchange that energy across subsequent half cycles. But since $v_{EMF.R}$ continues to source power, L_R and C_R's energy grows until D_{REC}, which a millivolt-drop FET can implement [11], clamps C_R to C_{REC}'s v_{REC}. Past that point, D_{REC} drains L_R into C_{REC}. C_R then discharges into L_R, and after v_C reaches zero, L_R drains into C_R to reduce v_C to a negative peak. After that, C_R drains into L_R and L_R back into C_R until, again, D_{REC} clamps and depletes L_R's leftover energy into C_{REC}. C_{REC} collects energy this way every other half cycle [7].

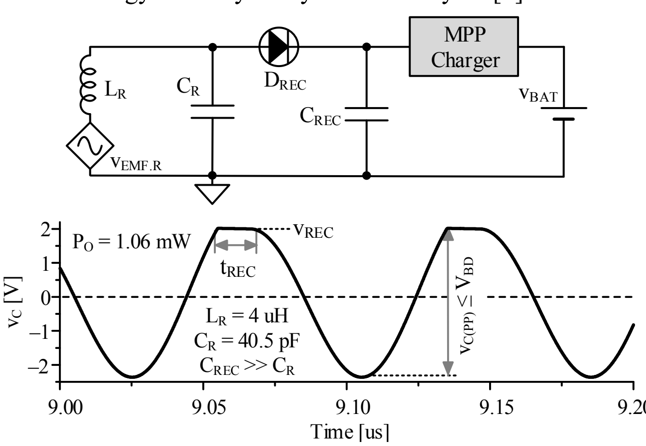

Fig. 3. Schematic and simulated response of the resonant half bridge.

Drawn Power: Considering the effects of drawn power on a distant transmitter are minimal, the receiver should draw as much power as possible. For that, since C_{REC} collects $v_{EMF.R}$'s i_L at v_{REC}, v_{REC} should be as high as possible. This is the purpose of the maximum power-point charger in Fig. 3, to draw just enough power to keep v_{REC} as high as the breakdown voltage V_{BD} allows. So to keep D_{REC} from breaking, C_R's peak–peak voltage $v_{C(PP)}$ should near, but not exceed V_{BD}.

Since $v_{EMF.R}$ in small distant coils is very low, and v_C swings to v_{REC} and C_R's energy at v_{REC} drains into L_R and back into C_R to swing v_C to $-v_{REC}$, $v_{EMF.R}$ is a negligible part of v_{REC} in v_C [10]. This means, energy in L_R and C_R is much greater than the energy $v_{EMF.R}$ delivers, so v_C swings close to $2v_{REC}$ to ensure, like v_{EXT} in Fig. 2, $v_{EMF.R}$ and i_L are in phase. As a result, L_R and C_R exchange energy and D_{REC} bleeds into C_{REC} once per cycle what $v_{EMF.R}$ supplies across both half cycles.

L_R's peak energy $E_{L(PK)}$ at $i_{L(PK)}$ therefore matches C_R's counterpart $E_{C(PK)}$ at $v_{C(PK)}$, so $i_{L(PK)}$ and $v_{C(PK)}$ relate:

$$E_{C(PK)} = 0.5C_R v_{C(PK)}^{\ 2} \approx E_{L(MAX)} = 0.5L_R i_{L(PK)}^{\ 2} \qquad (1)$$

$$i_{L(PK)} \approx v_{C(PK)}\sqrt{\frac{C_R}{L_R}}\ . \qquad (2)$$

With i_L's in-phase $i_{L(PK)}\sin(\omega_O t)$, $v_{EMF.R}$'s $v_{EMF.R(PK)}\sin(\omega_O t)$ is able to output EMF power $v_{EMF.R}i_L$ as P_{EMF}:

$$P_{EMF} \approx \frac{1}{T_O}\int_0^{T_O} v_{EMF.R} i_L\, dt = \frac{v_{EMF.R(PK)} v_{C(PK)}}{2}\sqrt{\frac{C_R}{L_R}}\ . \qquad (3)$$

But since D_{REC} suffers v_C's total swing $2v_{C(PK)}$, D_{REC}'s breakdown level V_{BD} limits $v_{C(PK)}$ and v_{REC} to $0.5V_{BD}$.

Output Power: Power losses, however, reduce how much power C_{REC} collects. Of possible losses, the ohmic power i_L's sinusoid burns in series resistances R_{SER} is usually dominant because tiny packages and skin effect elevate L_R's portion R_{ESR} to 5–10 Ω [12]. This overall $R_{SER}i_{L(RMS)}^2$ loss is

$$P_R = R_{SER}\, i_{L(RMS)}^{\ 2} \approx R_{SER}\left(\frac{i_{L(PK)}}{\sqrt{2}}\right)^2 \approx R_{SER}\left(\frac{v_{C(PK)}}{\sqrt{2}}\sqrt{\frac{C_R}{L_R}}\right)^2 . \qquad (4)$$

Note L_R's quality factor Q_R specifies R_{ESR} with $2\pi f_O L_R/R_{ESR}$.

Interestingly, P_{EMF} and P_R both climb with $v_{C(PK)}$. The system should therefore raise $v_{C(PK)}$ until the rise in ohmic loss P_R cancels the gain in P_{EMF}, which happens when the derivative of their difference is zero and $v_{C(PK)}$ is $v_{C(PK)}'$

$$\left.\frac{\partial\left(P_{EMF} - P_R\right)}{\partial v_{C(PK)}}\right|_{v_{C(PK)}' = \left(\frac{v_{EMF.R(PK)}}{2R_{SER}}\right)\sqrt{\frac{L_R}{C_R}}} \equiv 0\ . \qquad (5)$$

So barring other losses and limits, maximum power P_O' can be

$$P_O' \approx \left.\left(P_{EMF} - P_R\right)\right|_{v_{C(PK)} = v_{C(PK)}'} = \frac{v_{EMF.R(PK)}^{\ 2}}{8R_{SER}}\ . \qquad (6)$$

In practice, maximum output power is 1%–2% lower because bleeding energy from C_R clips v_C's sinusoid to a lower peak.

B. Resonant Full Bridge

C_R in the resonant full bridge of Fig. 4 [6] similarly produces a voltage v_C across C_R that, when tuned to $v_{EMF.R}$'s f_O, peaks between $v_{EMF.R}$'s half cycles. So $v_{EMF.R}$ supplies more power than it consumes and L_R and C_R receive and exchange that rising energy across half cycles until millivolt diodes [11] clamp C_R to v_{REC}. At that point, the diodes drain L_R into C_{REC}, C_R then drains into L_R, and L_R depletes back into C_R to reduce v_C to $-v_{REC}$. But since $v_{EMF.R}$ supplies energy across half cycles, L_R has leftover energy that the diodes bleed into C_{REC}. So after L_R depletes, C_R drains into L_R, L_R drains back into C_R to raise v_C to v_{REC}, and the cycle repeats. So in all, L_R and C_R exchange energy across half cycles and C_{REC} receives the energy $v_{EMF.R}$ supplies when C_R clamps to v_{REC} and to $-v_{REC}$.

Power: Since half and full bridges both resonate and clamp to a $v_{C(PK)}$ that dwarfs $v_{EMF.R}$, L_R and C_R exchange about the same energy and produce the same current. So with the same R_{SER}, they draw the same EMF power P_{EMF} and lose the same ohmic loss P_R to produce the same maximum power P_O' at the same $v_{C(PK)}'$. Operationally, the only difference is that the full bridge collects half the energy every half cycle that the half bridge collects every other half cycle.

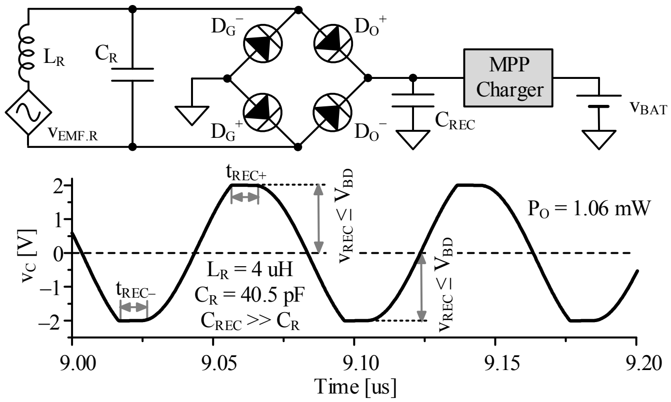

Fig. 4. Schematic and simulated response of the resonant full bridge.

Since ground diodes keep terminal voltages from dipping below 0 V, no terminal voltage in the circuit exceeds $v_{C(PK)}$'s v_{REC}. As a result, $v_{C(PK)}$ can be as high as breakdown level V_{BD}. This means, $v_{C(PK)}$ can be 2× that of the half bridge. By the way, if $v_{C(PK)}$ exceeds a MOS threshold voltage, cross-coupled FETs can replace D_G^+ and D_G^- or D_O^+ and D_O^- [13].

IV. Switched Bridges

A. Half-Switched Bridge

Replacing ground diodes in the resonant bridge with synchronous switches like Fig. 5 shows allows L_R to collect energy across half cycles and drain between half cycles [9]. For this, S_G^+ and S_G^- close to energize L_R from $v_{EMF.R}$ across half cycles. Then, near the end of the positive half cycle, S_G^- opens, and since L_R's i_L flows up at that time, D_O^+ drains L_R into v_{BAT}. At the end of the other half cycle, i_L flows in the opposite direction, so S_G^+ opens and D_O^- depletes L_R into v_{BAT}.

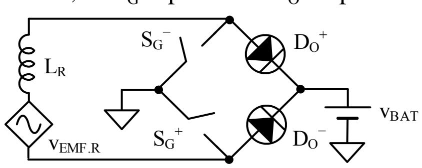

Fig. 5. Half-switched bridge.

The advantage of this configuration is that v_{BAT} has no bearing on i_L or $v_{EMF.R}$'s EMF power, so the system can charge v_{BAT} directly. This feature, however, is also its drawback because $v_{EMF.R}$ is so low that L_R's i_L is never far from zero. With such a low current, $v_{EMF.R}$ cannot supply much power.

B. Fully Switched Bridge

The aim of the fully switched bridge in Fig. 6 is to raise L_R's i_L to the highest level possible [10], [14]. For this, the switches connect a v_{REC} that is much greater than $v_{EMF.R}$ to L_R. Connecting v_{REC} across $v_{EMF.R}$'s first quarter cycle raises i_L to a high peak: to $i_{L(PK)}$ or $0.25v_{REC}T_O/L_R$. Reversing v_{REC} after that for another quarter cycle reduces i_L to zero and to $-i_{L(PK)}$ across yet another quarter cycle so that reversing v_{REC} can again raise i_L to zero at the end of the cycle. This way, $v_{EMF.R}$ and i_L are in phase and i_L is at the highest possible level.

Drawn Power: $v_{EMF.R}$'s power across every quarter cycle is the same because $v_{EMF.R}$ and i_L are in phase and symmetrical about zero every quarter cycle. Since v_{REC} dwarfs $v_{EMF.R}$, connecting v_{REC} across that time raises i_L at a rate of v_{REC}/L_R. With this changing i_L, $v_{EMF.R}$'s $v_{EMF.R(PK)}\sin(\omega_O t)$ supplies

$$P_{EMF} \approx \frac{1}{0.25T_O}\int_0^{0.25T_O} v_{EMF.R}\left(\frac{v_{REC}}{L_R}\right)t\,dt = \frac{v_{EMF.R(PK)}v_{REC}T_O}{\pi^2 L_R}. \quad (7)$$

The role of the maximum power-point charger is to keep v_{REC} at the highest possible level, near breakdown voltage V_{BD}.

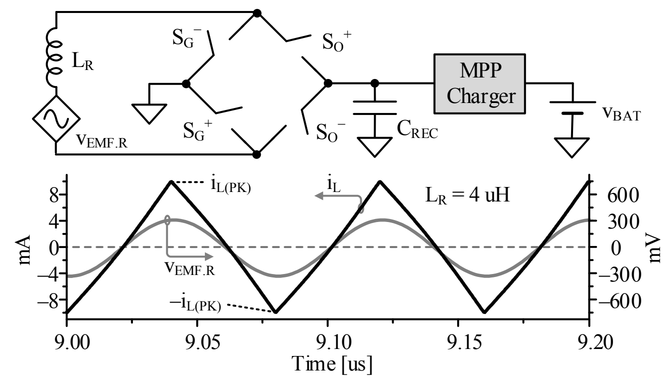

Fig. 6. Schematic and simulated response of the fully switched bridge.

Output Power: Power losses, however, reduce how much power C_{REC} collects. Of these, series ohmic power is usually dominant because tiny packages and skin effect keep L_R's R_{ESR} near 5–10 Ω [12]. Since i_L's triangular RMS current is $i_{L(PK)}/\sqrt{3}$ and $i_{L(PK)}$ is nearly $0.25T_O(v_{REC}/L_R)$, R_{SER}'s loss is

$$P_R = R_{SER}\, i_{L(RMS)}^{\ 2} \approx R_{SER}\left[\left(\frac{v_{REC}}{L_R}\right)\left(\frac{0.25T_O}{\sqrt{3}}\right)\right]^2. \quad (8)$$

Interestingly, P_{EMF} and P_R both climb with v_{REC}. The system should therefore raise v_{REC} until the rise in P_R cancels the gain in P_{EMF}, which happens when the derivative of their difference is zero and v_{REC} is v_{REC}'

$$\left.\frac{\partial(P_{EMF} - P_R)}{\partial v_{REC}}\right|_{v_{REC}' = \left(\frac{v_{EMF.R(PK)}}{R_{SER}}\right)\left(\frac{24L_R}{\pi^2 T_O}\right)} \equiv 0. \quad (9)$$

So barring other losses and limits, maximum power P_O' can be

$$P_O' \approx \left.(P_{EMF} - P_R)\right|_{v_{REC}=v_{REC}'} = \left(\frac{v_{EMF.R(PK)}^{\ 2}}{R_{SER}}\right)\left(\frac{12}{\pi^4}\right). \quad (10)$$

[14], however, sacrifices one of every 13 cycles to synchronize the switches to $v_{EMF.R}$'s quarter cycles, so maximum output power can be 7.7% lower than P_O'.

V. Switched Resonant Bridge

The switched resonant bridge in Fig. 7 [12] closes S_R to, like the resonant bridge, resonate L_R and C_R; but unlike the resonant bridge, sometimes opens S_R to drain L_R and C_R *in series*. Like before, C_R produces a voltage v_C that, when tuned to $v_{EMF.R}$'s f_O, peaks between $v_{EMF.R}$'s half cycles. So $v_{EMF.R}$ supplies more power than it consumes and L_R and C_R receive and exchange that rising energy across half cycles to the point v_C dwarfs $v_{EMF.R}$. When $v_{C(PK)}$ reaches its maximum power point, S_R opens and the diodes drain L_R's leftover energy into v_{BAT}. S_R then closes to drain C_R at $v_{C(PK)}$ into L_R and L_R back into C_R so v_C reaches $-v_{C(PK)}$, past which point S_R opens. But since $v_{EMF.R}$ supplied L_R across this time, the diodes deplete L_R's leftover energy into v_{BAT}. S_R then closes to drain C_R into L_R and L_R back into C_R until v_C reaches $v_{C(PK)}$. After that, S_R opens and L_R again drains into v_{BAT} to start another cycle.

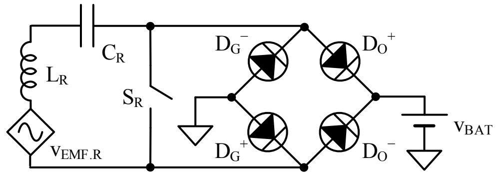

Fig. 7. Switched resonant bridge.

Power: Since switched and non-switched resonant bridges resonate to a voltage that dwarfs $v_{EMF.R}$, L_R and C_R exchange about the same energy and produce the same current. So with the same R_{SER}, drawn EMF power and lost ohmic power match to produce the same maximum power at the same peak voltage. An MPP charger, however, is not necessary because the bridge's rectified output does not limit v_C's swing. And since S_R and the diodes keep all terminal voltages between 0 V and v_{BAT}, v_C can swing as high as C_R allows. So when C_R is off chip, v_C can swing to C_R's off-chip breakdown level, which can be considerably greater than that of S_R and the bridge [15].

VI. Comparison

A power receiver draws the most EMF power from a tiny under-damped coil when i_L is in phase with $v_{EMF.R}$ and at the highest possible level. For this, C_R in resonant bridges impresses across L_R a sinusoidal voltage that peaks to v_{REC}. But since C_{REC} in a switched bridge keeps L_R's voltage steady at v_{REC}, i_L is higher in the switched bridge, so P_{EMF} in Fig. 8 is 27% higher at 2–15 V than for resonant bridges.

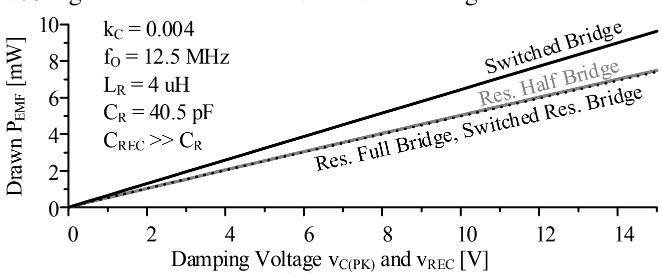

Fig. 8. Simulated EMF power drawn.

Since all resonant bridges resonate the same way, drawn, lost, and output power all match, so output power maxes at the same level with the same peak voltage, at 1.6 mW with 6.2 V in Fig. 9. Although the switched bridge draws more EMF power, its higher current burns more ohmic power to limit output power to about the same level.

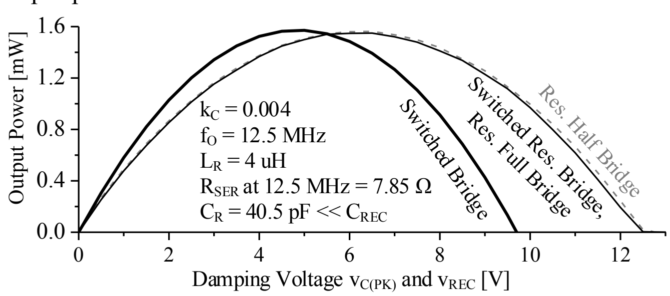

Fig. 9. Simulated output power.

VII. Conclusions

Although all resonant and switched bridges *can* output about as much power, breakdown voltages and losses limit the switched resonant bridge to a lesser extent than others. Plus, removing the MPP charger that others require for maximum power saves space. Outputting higher power with less volume this way is crucial when space is scarce and coils are centimeters apart. True, when within millimeters, the receiver can over-damp the transmitter before losses can limit the receiver. So short a distance, however, is rare for embedded microsensors.

Acknowledgment

The authors thank Paul Emerson, Dr. Rajarshi Mukhopadhyay, Dr. Orlando Lazaro, and Texas Instruments for their support, feedback, and sponsorship.

References

[1] P.J. Chen D.C. Rodger, S. Saati, *et al.*, "Implantable parylene-based wireless intraocular pressure sensor," *IEEE International Conference on Micro Electro Mechanical Systems*, pp. 58-61, Jan. 2008.

[2] M.A. Fonseca, J.M. English, M.V. Arx, and M.G. Allen, "Wireless micromachined ceramic pressure sensor for high-temperature applications," *IEEE J. Microelectromechanical Systems*, vol. 11, no. 4, pp. 337-343, Aug. 2002.

[3] N. Cho, S.J. Song, S. Kim, *et al.*, "A 5.1-µW UHF RFID tag chip integrated with sensors for wireless environmental monitoring," *IEEE European Solid-State Circuits Conference*, pp. 279-282, Sept, 2005.

[4] H.A. Sodano, D.J. Inman, and G. Park, "Comparison of piezoelectric energy harvesting devices for recharging batteries," *J. Intelligent Material Systems and Structures*, vol. 16, no. 10, pp. 799-807, Oct. 2005.

[5] S. Chalasani and J.M. Conrad, "A survey of energy harvesting sources for embedded systems," *IEEE Southeastcon*, pp. 442-447, April 2008.

[6] S.B. Lee, H.M. Lee, M. Kiani, *et al.*, "An inductively-powered scalable 32-channel wireless neural recording system-on-a-chip for neuroscience applications," *IEEE Trans. on Biomedical Circuits and Systems*, vol. 4, no. 6, pp. 360-371, Dec. 2010.

[7] R.R. Harrison, P. T. Watkins, R. J. Kier, *et al.*, "A low-power integrated circuit for a wireless 100-electrode neural recording system," *IEEE J. of Solid-State Circuits,* vol. 42, no. 1, pp. 123-133, Jan. 2007.

[8] I. Mayordomo, T. Drager, J.A. Alayon, *et al.*, "Wireless power transfer for sensors and systems embedded in fiber composites," *IEEE Wireless Power Transfer*, pp. 107-110, May 2013.

[9] O. Lazaro and G.A. Rincón-Mora, "180-nm CMOS wideband capacitor-free inductively coupled power receiver and charger," *IEEE J. of Solid-State Circuits*, vol. 48, no. 11, pp. 2839-2849, Nov. 2013.

[10] O. Lazaro and G.A. Rincón-Mora, "Inductively coupled 180-nm CMOS charger with adjustable energy-investment capability," *IEEE Trans. on Circuits and Systems II,* vol. 60, no. 8 pp. 482-486, July 2013.

[11] S.Y. Lee, M.Y. Su, M.C. Liang, *et al.*, "A programmable implantable micro-stimulator SoC with wireless telemetry: Application in closed-loop endocardial stimulation for cardiac pacemaker," *IEEE Trans. on Biomedical Circuits and Systems*, vol. 5, no. 6, pp. 511-522, Dec. 2011.

[12] M. Kiani, B. Lee, P. Yeon, and M. Ghovanloo, "A Q-Modulation Technique for Efficient Inductive Power Transmission", *IEEE J. Solid-States Circuits*, vol. 99, pp. 1-10, July 2015.

[13] C. Peters, J. Handwerker, D. Maurath, *et al.*, "A sub-500 mV highly efficient active rectifier for energy harvesting applications," *IEEE Trans. on Circuits and Systems I*, vol. 58, no. 7, 1542-1550, July 2011.

[14] O. Lazaro and G.A. Rincón-Mora, "A non-resonant self-synchronizing inductively coupled 0.18-um CMOS power receiver and charger," *IEEE J. of Emerging and Selected Topics in Power Electronics*, vol. 3, no. 1, pp. 261-271, Mar. 2015.

[15] W. J. Sarjeant, J. Zirnheld, and F. W. MacDougall, "Capacitors," *IEEE Trans. Plasma Science*, vol. 26, no. 5, pp. 1368-1392, Oct. 1998.